Pro-oxidant activity of aluminum: Promoting the Fenton reaction by reducing Fe(III) to Fe(II)

ARTICLE *in* JOURNAL OF INORGANIC BIOCHEMISTRY · SEPTEMBER 2012

Impact Factor: 3.44 · DOI: 10.1016/j.jinorgbio.2012.09.008 · Source: PubMed

Journal of Inorganic Biochemistry 117 (2012) 118–123

Contents lists available at SciVerse ScienceDirect

Journal of Inorganic Biochemistry

journal homepage: www.elsevier.com/locate/jinorgbio

Pro-oxidant activity of aluminum: Promoting the Fenton reaction by reducing Fe(III) to Fe(II)

F. Ruipérez [a,*], J.I. Mujika [a], J.M. Ugalde [a], C. Exley [b], X. Lopez [a]

[a] Kimika Fakultatea, Euskal Herriko Unibertsitatea (UPV/EHU) and Donostia International Physics Center (DIPC), P. K. 1072, 20080 Donostia, Euskadi, Spain
[b] Birchall Centre for Inorganic Chemistry and Materials Science, Keele University, Staffordshire, UK

ARTICLE INFO

Article history:
Received 10 April 2012
Received in revised form 3 September 2012
Accepted 3 September 2012
Available online 12 September 2012

Keywords:
Theoretical study
Aluminum superoxide
Pro-oxidant activity
Fenton reaction
Fe(III) reduction

ABSTRACT

The possibility for an Al-superoxide complex to reduce Fe(III) to Fe(II), promoting oxidative damage through the Fenton reaction, is investigated using highly accurate ab initio methods and density functional theory in conjunction with solvation continuum methods to simulate bulk solvent effects. It is found that the redox reaction between Al-superoxide and Fe(III) to produce Fe(II) is exothermic. Moreover, the loss of an electron from the superoxide radical ion in the Al-superoxide complex leads to a spontaneous dissociation of molecular oxygen from aluminum, recovering therefore an Al^{3+} hexahydrated complex. As demonstrated in previous studies, this complex is again prone to stabilize another superoxide molecule, suggesting a catalytic cycle that augments the concentration of Fe(II) in the presence of Al(III). Similar results are found for $Al(OH)^{2+}$ and $Al(OH)_2^+$ hydrolytic species. Our work reinforces the idea that the presence of aluminum in biological systems could lead to an important pro-oxidant activity through a superoxide formation mechanism.

1. Introduction

Aluminum, the most abundant metal in the earth's crust, has largely been excluded from biochemical evolution because of its efficient cycling within the lithosphere [1,2]. However, human intervention (soil acidification, food additives, pharmaceuticals, Al-containers,...) has increased the availability of biologically reactive aluminum [2,3]. Its presence has been linked to various human diseases [4–6], although the exact mechanisms for aluminum toxicity are still unknown. A first step towards its understanding is the characterization of aluminum speciation in biosystems.

Aluminum is able to form a variety of strong complexes with diverse bioligands, including high molecular mass (HMM) proteins such as transferrin [7], and low molecular mass (LMM) molecules such as citrate [8,9]. The characterization of Al(III) speciation in biosystems is a complex problem, and theoretical calculations can help shed light on the different Al-complexes formed in aqueous solution at equilibrium [8–19] and non-equilibrium [20,21]. In this sense, calculations show [9,18,22] that Al^{3+} can deeply alter the structural and chemical properties of bound ligands, pointing to a significant interference of Al^{3+} in biological systems. Additional reported bioeffects of Al include interaction with phosphates such as ADP and ATP [3], and enhancement of ROS (reactive oxygen species) production [5].

Although most aluminum is complexed in a bioenvironment, nanomolar amounts of aluminum are exchangeable and compete effectively with mM amounts of essential metals, in particular magnesium and iron [24]. For example, aluminium has been shown to replace magnesium in the catalytic sites of regulatory enzymes [3,4,25–27], and model calculations have shown that Al^{3+} can displace Mg^{2+} in carboxylic-rich buried metal sites [13–15,18,23]. Aluminum also competes effectively with ferric iron, due to its same charge and similar ionic radii with their favoured octahedral coordination [24]. These properties allow aluminum to mimic iron and to bind to the iron transport protein, transferrin [28], and to iron regulatory protein mRNA [29], consequently disrupting iron metabolism in cells. It is also well established that there is a net accumulation of aluminum in the human brain that increases with aging, particularly affecting some neurons in certain vulnerable regions of aged Alzheimer-affected brains [30–32].

Aluminum exhibits a significant pro-oxidant activity, promoting biological oxidation both in-vitro and in-vivo [33,34]. The formation of an Al-superoxide ($O_2^{\bullet -}$ radical) complex has been hypothesized [35] to be central to this oxidant activity. In this vein, Fukuzumi et al. [36–38] have shown that there exists a linear relationship between the strength of a metal-superoxide interaction and the oxidant activity displayed by the metal. In a recent publication [39], we determined that in the case of aluminum: *i)* there is a strong intrinsic interaction with superoxide, *ii)* the strength of this interaction is larger than for common biometals, *iii)* microsolvation does not alter the relative strength of this interaction with respect to biometals and *iv)* the formation of a complex between Al^{3+} and $Al(OH)^{2+}$ with a superoxide radical anion in aqueous solvent is highly favored thermodynamically.

In the present paper, we investigate the possibility for Al-superoxide complexes to induce oxidation of biomolecules by enhancing Fe(II) concentration over Fe(III). This would promote Fenton reaction in systems

* Corresponding author.
E-mail address: fernando.ruiperez@gmail.com (F. Ruipérez).

0162-0134/$ – see front matter © 2012 Elsevier Inc. All rights reserved.
http://dx.doi.org/10.1016/j.jinorgbio.2012.09.008

in-vivo, therefore increasing the concentration of important biooxidants such as $^{\bullet}OH$ radical. For this purpose, highly accurate theoretical methods are used, including wavefunction-based calculations, such as CASSCF and CASPT2, and density functional theory (DFT) with various functionals. In addition, bulk solvent effects are incorporated by continuum models. We show that aluminum-superoxide complexes in different forms considered in the present paper, namely $[Al(O_2^{\bullet})(H_2O)_5]^{2+}$, $[Al(O_2^{\bullet})(OH)(H_2O)_4]^{+}$ and $[Al(O_2^{\bullet})(OH)_2(H_2O)_3]$, have a high potentiality to reduce Fe(III) to Fe(II). Our results, therefore, support the hypothesis of promotion of Fenton reaction by Al(III).

2. Methods

2.1. Density functional theory calculations

All geometrical optimizations were carried out in gas phase using the Gaussian 09 suite of programs [40] employing B3LYP functional [41–44] in conjunction with the 6-31++g(d,p) basis set. To confirm that the optimized structures were minima on the potential energy surfaces, frequency calculations were carried out at the same level of theory. All structures showed real frequencies for all the normal modes of vibration. The frequencies were then used to evaluate the zero-point vibrational energy (ZPVE) and the thermal (T = 298 K) vibrational corrections to the enthalpy and Gibbs free energy in the harmonic oscillator approximation. To calculate the entropy, the different contributions to the partition function were evaluated using the standard expressions for an ideal gas in the canonical ensemble and the harmonic oscillator and rigid rotor approximation. The electronic energy was refined by single-point energy calculations at the B3LYP/6-311++G(3df,2p) level of theory. Moreover, the reliability of B3LYP functional has been verified by single-point calculations using the PBE0 [45] and M06-2X DFT [46] functionals and the 6-311++G(3df,2p) basis set.

2.2. CASSCF and CASPT2 calculations

Wavefunction-based calculations were performed at the all-electron level with scalar relativistic effects included by using the second-order Douglas-Kroll-Hess Hamiltonian [47,48]. The wavefunctions were obtained by means of complete active space self-consistent field calculations (CASSCF) [49–51], which mainly recover the non-dynamic or static correlation, while the dynamic correlation was taken into account through complete active space second-order perturbation theory calculations (CASPT2) [52,53]. The active space used to obtain the CASSCF wavefunctions in Fe(II) compounds consists of 10 electrons distributed in 12 molecular orbitals (9 electrons in 12 molecular orbitals in the case of Fe(III) compounds), that is, the five iron 3d orbitals plus a second 4d shell to describe the so-called double-shell effect [54], and two bonding ligand orbitals. The core 1s electrons from oxygen as well as the iron 1s-2p atomic shells were kept frozen in the subsequent CASPT2 calculations. The imaginary shift technique [55], with a value of 0.10 a.u., was used to achieve convergence and avoid the presence of intruder states in this step. In the Al-superoxide calculations, the active space is defined by the distribution of 13 electrons in 9 molecular orbitals from the $O_2^{\bullet -}$ unit: σ_{2s}, σ_{2s}^*, π_{2px}, π_{2py}, π_{2px}^*, π_{2py}^*, σ_{2pz}, and σ_{2pz}^*, and the 3s orbital from Al. In the CASPT2 step, the inner 2s and 2p orbitals from aluminum are also correlated. An imaginary shift of 0.20 a.u was used. All CASSCF/CASPT2 calculations were performed with MOLCAS 7.4 suite of programs [56]. We have used the all-electron atomic natural orbitals (ANO-RCC) basis sets of quadruple-ζ size for all atoms plus one *h* polarization function in Fe, with the following primitives and contractions: on iron (21s15p10d6f4g2h)/[7s6p5d3f2g1h] [57], on aluminum (17s12p5d3f2g)/[6s5p3d2f] [58], on oxygen (14s9p4d3f2g)/[5s4p3d2f] [58] and finally, on hydrogen (8s4p3d1f)/[4s3p2d] [59].

2.3. Bulk solvent effects

Two alternative procedures were followed to estimate the solvation free energies of the gas-phase B3LYP/6-31++G(d,p) geometries using the self-consistent reaction field (SCRF) method. In the first one, denoted as ΔG_{solv}^{PCM}, the polarizable continuum model (PCM) approach [60–63] was employed using the united atom Hartree-Fock (UAHF) set of atomic radii to build the cavity. These radii have been optimized with the HF/6-31G(d) wavefunction to give accurate solvation free energies of a dataset of anionic/cationic and neutral organic and inorganic molecules [61]. Therefore, the HF/6-31G(d) level of theory was chosen to represent the solute. In the second one, ΔG_{solv}^{SMD} the solvation model density (SMD), a universal solvation model developed by Truhlar et al. [64], was employed at the B3LYP/6-311++g(3df,2p) level of theory.

Thus, the final free energy in aqueous solvent (G_{aq}) for each structure was evaluated, following standard procedures, [65] as: $G_{aq} = E_{electr} + ZPVE + E^{therm} - T{\cdot}S + \Delta G_{solv}$, where E_{electr} stands for the B3LYP/6-311++G(3dp,2p) electronic energy in the gas-phase calculated by either of the methods described in sections 2.1 and 2.2, ZPVE the zero-point vibrational energy, E^{therm} the thermal energy contribution, T the temperature (298 K), S the entropy contribution at T = 298 K, and ΔG_{solv}, the solvation free energy, is determined with either PCM or SMD.

3. Results and discussion

3.1. Calibration of the method

In this section, in order to calibrate the accuracy of the density functionals used in this work, we compare the ionization energies (Table 1) obtained for Fe^{2+} and AlO_2^{2+} using B3LYP, PBE and M062X functionals with highly accurate CASPT2 calculations, and experimental numbers when available. For the bare Fe^{2+} ion in the gas phase, the experimental ionization energy is 705.6 kcal/mol, and CASPT2 shows an outstanding agreement, 704.2 kcal/mol, whereas DFT methods present larger deviations, 714.2–728.7 kcal/mol, with the largest error corresponding to B3LYP. Upon microsolvation, the differences in ionization energies among the different methods are reduced, and DFT numbers (383.6–386.4 kcal/mol) are similar to the CASPT2 one (379.6 kcal/mol). Again, the largest difference corresponds to B3LYP, but the absolute error with respect to CASPT2 is now reduced to 6.8 kcal/mol. Introduction of a second shell of waters (See Fig. 1) was only possible at DFT level of theory due to computational limitations, obtaining a similar ionization energy for the three DFT functionals, ranging from 281.5 kcal/mol (PBE) to 286.5 kcal/mol (B3LYP). Previous calculations performed using DFT and local density approximation, LDA, obtained a value of 386.9 kcal/mol for the microsolvated structures

Table 1
Ionization energies of Fe^{2+} and AlO_2^{0+} for the bare ions and with water coordination shell. Values in kcal/mol.

	B3LYP	PBE	M062X	CASPT2	Exp.
$Fe^{2+} \rightarrow Fe^{3+}$					
Bare ion	728.7	719.5	714.2	704.2	705.6[a]
$Fe(H_2O)_6^{2+} \rightarrow Fe(H_2O)_6^{3+}$	386.4	382.7	383.6	379.6	
$Fe(H_2O)_6(H_2O)_{12}^{2+} \rightarrow Fe(H_2O)_6(H_2O)_{12}^{3+}$	286.5	281.5	283.6	–	
$AlO_2^{2+} \rightarrow AlO_2^{3+}$					
$AlO_2^{2+} \rightarrow AlO_2^{3+}$	593.0	589.4	588.5	570.7	
$Al(O_2^{\bullet})(H_2O)_5^{2+} \rightarrow Al(O_2)(H_2O)_5^{3+}$	366.3	363.9	366.1	365.0	
$Al(O_2^{\bullet})(H_2O)_5(H_2O)_{12}^{2+} \rightarrow Al(H_2O)_6(O_2)(H_2O)_{11}^{3+}$	276.4	274.0	283.5	–	

[a] Ralchenko, Yu., Kramida, A.E., Reader, J., and NIST ASD Team (2011). NIST Atomic Spectra Database (ver. 4.1.0), [Online]. Available: http://physics.nist.gov/asd3 [2011, June 29]. National Institute of Standards and Technology, Gaithersburg, MD.

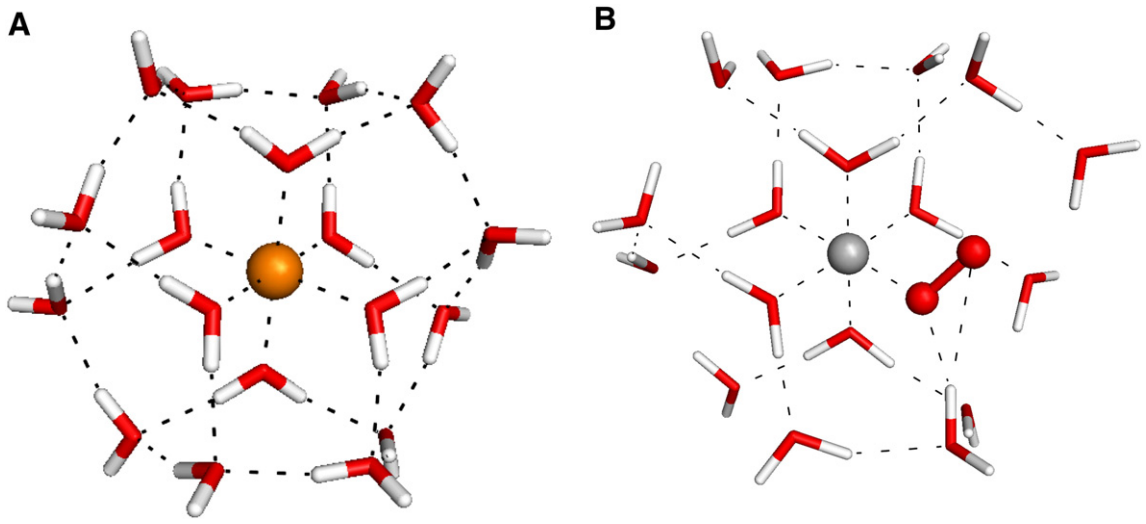

Fig. 1. Microsolvated structure of Fe^{2+} and $AlO_2^{\bullet 2+}$ with first and second coordination shells considered.

and of 268.2 kcal/mol including a second shell of water molecules (for more details see Ref. [66]).

In the case of the Al-superoxide complex, a similar trend is observed. In general, larger ionization energies are obtained for DFT methods than for CASPT2, but the differences among the methods are lowered as we consider microsolvated structures. For our largest models, which include first and second solvation water molecules, we obtain values for the ionization energies that are within 5 kcal/mol for the different functionals. There are two important remarks to be made about these calculations, upon ionization of $AlO_2^{\bullet 2+}$ and formation of molecular oxygen, we observed that the $Al(O_2)^{3+}$ complex changes its ground spin state as a function of microsolvation. Thus, whereas the bare $Al(O_2)^{3+}$ complex showed a singlet ground state, the microsolvated $Al(O_2)(H_2O)_5^{3+}$ and $Al(O_2)(H_2O)_5(H_2O)_{12}^{3+}$ structures showed a triplet ground state. On the other hand, upon ionization of the $Al(O_2^{\bullet})(H_2O)_5(H_2O)_{12}^{+2-}$ complex, we observed a spontaneous exchange between the molecular oxygen and one of the second shell water molecules, therefore the resultant structure does not show a direct interaction between Al and oxygen and it is better described as $Al(H_2O)_6(O_2)(H_2O)_{11}^{3+}$. Irrespective of the method and of the type of structure, the ionization energies for the Al-superoxide complex are smaller than for Fe^{2+}, suggesting a thermodynamically favorable electron transfer from Al-superoxide complex to Fe^{3+} for both bare ion and microsolvated structures. In terms of methodologies, the present DFT functionals are accurate enough as to give meaningful results.

3.2. Reduction of Fe(III) to Fe(II) by Al^{3+}

Taking into account the adequacy of the theoretical protocol used, next we evaluate the thermodynamics of the following redox reaction: $Fe^{3+} + AlO_2^{\bullet 2+} \rightarrow Fe^{2+} + AlO_2^{3+}$, in which $Fe^{3+}$is being reduced by an Al-superoxide complex. The results are summarized in Table 2. Bulk solvent effects were also considered and added to the gas-phase B3LYP energetic data. In the gas phase, the redox reaction is highly favorable, but the exothermicity of the reaction is grately influenced by the number of solvation shells around the ions. Thus, upon introducing first-shell coordination water molecules, the redox reaction is still exothermic, but the exothermicity has decreased by one order of magnitude (−14.6/−20.1 kcal/mol). Introducing a second shell of water molecules leads to lower exothermicities, −10.1 kcal/mol at B3LYP. However, as commented in the previous section, the molecular oxygen does not interact directly with Al, and it has exchanged with one of the second shell water molecule, leading to the following structure $Al(H_2O)_6(O_2)(H_2O)_{11}^{3+}$. This suggests an spontaneous departure of the molecular oxygen upon loss of an electron from the superoxide. Entropic contributions tend to increase the exothermicity of the redox reaction, however bulk solvent effects has the opposite tendency and, depending on the solvation model, we obtain either an exothermic reaction by −9.9 kcal/mol or an endothermic one by 4.4 kcal/mol.

The departure of the molecular oxygen from the aluminum first coordination shell suggests that the overall redox reaction corresponds to $Fe^{3+} + AlO_2^{\bullet 2+} \rightarrow Fe^{2+} + Al^{3+} + O_2$. The results for this reaction can be found in Table 2. The exothermicity of the redox reaction, in solvated structures, has clearly augmented, highlighting the spontaneous dissociation of molecular oxygen from the Al^{3+} ion. At our best models, with explicit first and second coordination shell water molecules and bulk solvent effects, the reaction is clearly exothermic, with values of −19.8 kcal/mol and −7.4 kcal/mol for the two bulk solvation models considered (SMD and PCM, see methods).

Table 2
Redox reaction energies (ΔE) and free energies (ΔG) in kcal/mol, in gaseous and aqueous phases, for reduction of Fe(III) to Fe(II) from Al-superoxide complexes. ΔG_g is obtained using the B3LYP functional and ΔG_{aq}^{X} is calculated as $\Delta G_g + \Delta\Delta G_{solv}^{X}$ (X = PCM, SMD).

	ΔE						
	B3LYP	PBE	M062X	CASPT2	ΔG_g	ΔG_{aq}^{SMD}	ΔG_{aq}^{PCM}
$Fe^{3+} + AlO_2^{\bullet 2+} \rightarrow Fe^{2+} + AlO_2^{3+}$							
Bare ion	−135.7	−130.1	−125.7	−116.2			
First shell	−20.1	−18.8	−17.5	−14.6	−26.4	−2.9	16.6
Second shell[a]	−10.1	−7.5	0.0		−21.0	−9.9	4.4
$Fe^{3+} + AlO_2^{\bullet 2+} \rightarrow Fe^{2+} + Al^{3+} + O_2$							
Bare ion	−51.0	−49.2	−45.5				
First shell	−60.2	−60.8	−61.9		−64.2	−31.9	−47.2
Second shell	−42.0	−41.3	−39.6		−39.1	−19.8	−7.4
$Fe^{3+} + Al(OH)O_2^{\bullet})^{+} \rightarrow Fe^{2+} + Al(OH)^{2+} + O_2$							
Bare ion	−277.7	−216.4	−203.0				
First shell	−145.3	−146.5	−147.2		−149.0	−24.2	−14.8
Second shell	−101.4	−100.0	−97.5		−104.9	−19.2	−9.2
$Fe^{3+} + Al(OH)_2(O_2^{\bullet}) \rightarrow Fe^{2+} + Al(OH)_2^{+} + O_2$							
Bare ion	−491.6	−484.5	−472.4				
First shell	−248.3	−248.5	−249.1		−252.3	−33.5	−26.1
Second shell	−171.9	−172.8	−176.7		−171.2	−18.9	−12.1

[a] In AlO_2^{3+}, the O_2 molecule is not bound directly to Al.

Quite remarkably, our gas-phase data with the three different functionals show very small differences for this reaction energy, within 2.0 kcal/mol, indicating that the main conclusions of these calculations are unlikely to be affected by higher levels of theory.

3.3. Redox reactions from other hydrolytic species

Aluminum can coexist in a variety of hydrolytic species as a function of pH, although $Al^{3+}$is predominant at acidic pH's (pKa around 5.2). In our recent paper on Al-superoxide complexes, we analyzed the possibility of Al-superoxide formation from a variety of these hydrolytic species [39]. In particular, $Al(OH)^{2+}$, (more precisely, $Al(OH)(H_2O)_5^{2+}$), which shows an important concentration in the 4–5 pH range, showed a high thermodynamic tendency towards formation of an $Al(OH)(O_2^{\bullet})(H_2O)_4^{+}$ complex. Besides, $Al(OH)_2^{+}$ (significant in the 5–6.5 pH range) also showed a mild exothermic reaction towards $Al(OH)_2(O_2^{\bullet})(H_2O)_3$, although much more moderate. Therefore, we decided to investigate the possibility of a redox reaction departing from the $Al(OH)(O_2^{\bullet})^{+}$ and $Al(OH)_2(O_2^{\bullet})$ complexes. As seen in Table 2, in gas phase the capacity of these complexes to reduce Fe^{3+} to Fe^{2+} is higher as the charge of the Al-superoxide complex decreases. However, solvation tends to ameliorate these differences, as they are more unfavorable as the charge of the Al-superoxide decreases. After all contributions are added, we obtain final exothermicities that are very similar to the ones described for the AlO_2^{2+} complex, −19.2/−9.2 kcal/mol for $Al(OH)(O_2^{\bullet})^{+}$ and −18.9/−12.1 for $Al(OH)_2(O_2^{\bullet})$.

3.4. Fenton promotion cycle by Al(III)

In summary, AlO_2^{2+}, $Al(OH)(O_2^{\bullet})^{+}$ and $Al(OH)_2(O_2^{\bullet})$ complexes are able to reduce Fe^{3+} to Fe^{2+}. Taking into account the high thermodynamic tendency to form Al-superoxide complexes for Al^{3+} and $Al(OH)^{2+}$, and to a lesser extent for $Al(OH)_2(O_2^{\bullet})^{+}$, it implies that Al can exert a significant pro-oxidant activity by increasing the amount of Fe^{2+} in solution and promoting radical formation through the Fenton reaction. Thus, we could think of the following Fenton promotion cycle by aluminum (See Fig. 2). Let us consider first an Al^{3+} hydrolytic species. In our previous publication [39], we determined that Al^{3+} stabilizes the superoxide and forms an AlO_2^{2+} complex, by an exothermic reaction of −8.3/−15.2 kcal/mol (depending on the solvation model considered to include bulk solvent effects). Once the $AlO_2^{\bullet 2+}$ complex is formed, in the present paper we have determined that there is a favorable redox reaction that leads to the reduction of Fe^{3+} to Fe^{2+}, with an exothermicity of −19.8/−7.4 kcal/mol. This electron transfer also provokes the loss of direct interaction between oxygen and aluminum, due to the low affinity of a non-polar, neutral molecule such as O_2 towards a hard ion such as Al^{3+}, and therefore, leads to the spontaneous dissociation of molecular oxygen from aluminum, recovering the initial Al^{3+} species. As a result of these reactions, there is an increase of the concentration of Fe^{2+}. This metal ion is able to produce important oxidant species such as $^{\bullet}OH$ through the Fenton reaction, recovering back Fe^{3+}. On the other hand, the free molecular oxygen can capture another electron and form a superoxide, which in turn can be stabilized by Al^{3+}, and the whole cycle can start again. Our hypothesis of a Fenton promotion cycle by Al(III) is consistent with the previous evidence that aluminum reduces iron(III) to iron(II), the soluble form that drives the Fenton reaction [70].

Analogous promotion cycles can be also proposed for $Al(OH)^{2+}$, since both superoxide formation [39] (−8.7/−13.5 kcal/mol) and redox reaction of $Al(O_2^{\bullet})(OH)^{+}$ (−19.2/−9.2 kcal/mol) are highly favorable. A less favorable but possible promotion cycle could also be proposed for $Al(OH)_2^{+}$. The exothermicities for $Al(O_2^{\bullet})(OH)_2$

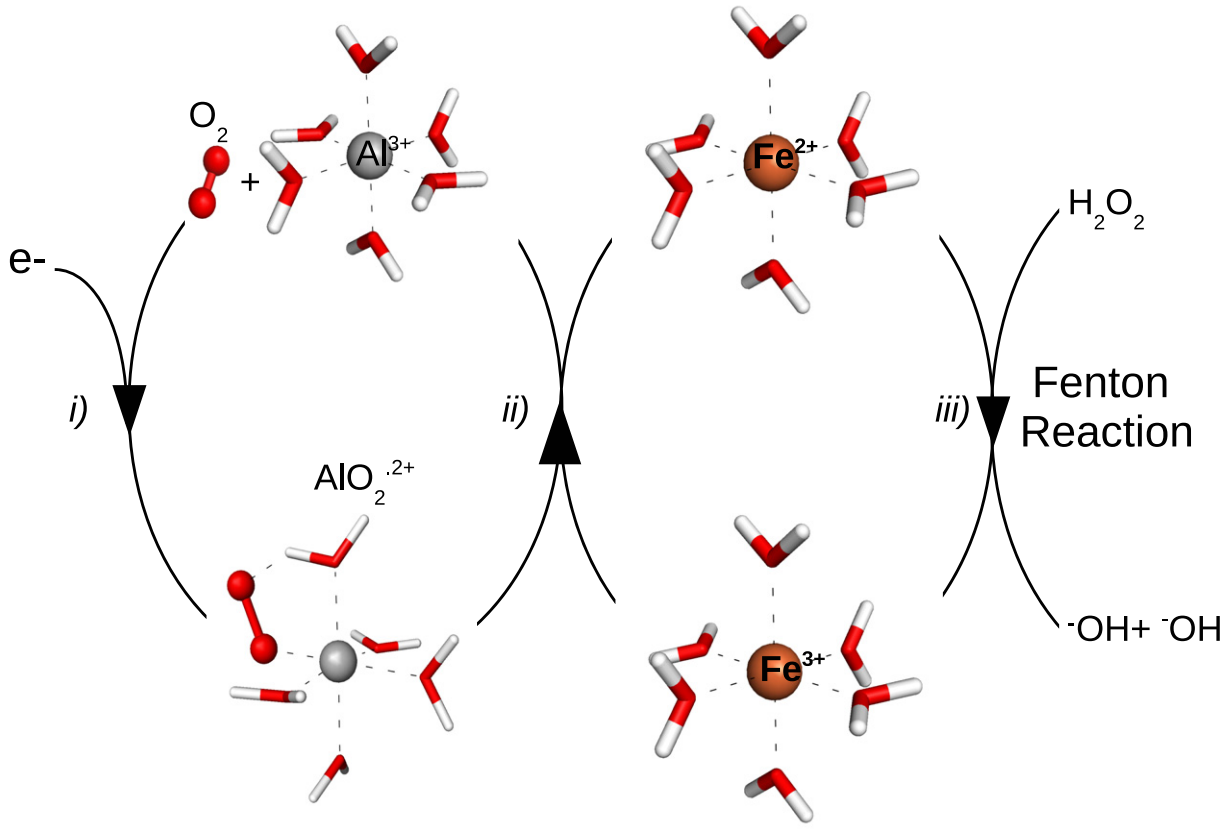

Fig. 2. Al^{3+} Fenton promotion cycle: *i)* Al^{3+} stabilizes a superoxide, forming an Al-superoxide complex; *ii)* Al-superoxide reduces Fe^{3+} to Fe^{2+}, leading to a spontaneous dissociation of molecular oxygen from aluminum and recovering the initial Al^{3+} species; *iii)* Fe^{2+} oxidizes back to Fe^{3+} by the Fenton reaction, inducing the formation of radicals ($^{\bullet}OH$) that causes oxidative damage. At the end of the process, the initial Al^{3+} and Fe^{3+} species are recovered.

formation are much lower, namely −1.7/−2.8 , and we can not rule out that higher levels of theory would change the sign of the reaction energy. Nevertheless, this data suggests that an Al-superoxide complex can be formed from $Al(OH)^{2+}$ species, and based on the reaction energies for the redox process, the resultant complex can also promote Fe(III) reduction. For other hydrolytic species, $Al(OH)_3$ and $Al(OH)_4^-$ the promotion cycle is not very likely for different reasons. The low solubility of $Al(OH)_3$ prevents for having significant concentrations in solution, although we characterized [39] an slightly exothermic reaction for Al-superoxide formation. On the other hand, in the case of $Al(OH)_4^-$, it is very unlikely that a superoxide can displace an hydroxide, and therefore no superoxide stabilization can be attained with this hydrolytic species.

The biological significance of the catalysis of Fenton chemistry by Al-superoxide complexes has recently been highlighted in describing the putative neurotoxicity of aluminum in conditions such as Alzheimer's and Parkinson's disease [67]. Aluminum has long been known to increase iron-induced oxidative reactions several-fold in liposomes, and physical systems over that which occurs in the absence of aluminum [71–73]. We have already shown that aluminum catalyses the reduction of Fe^{3+} to Fe^{2+} in vitro and that this 'equilibrium' is pushed even further towards Fe^{2+} in the additional presence of $A\beta_{42}$, the amyloidogenic peptide implicated in the amyloid cascade hypothesis of Alzheimer's disease [34]. This property of aluminum, and hence Al-superoxide, may explain a burgeoning number of observations of anomalous redox-active iron in neurodegenerative disease [68,69]. It may also begin to elucidate a mechanism for the formation of magnetic iron compounds associated with amyloid deposition and senile plaques in Alzheimer's disease [74–76]. The mechanism(s) by which these phenomena occur requires clarification and this paper raises a possible mechanism open to discussion.

4. Conclusions

Density functional theory and wavefunction-based methods such as CASSCF/CASPT2, in conjunction with continuum solvation models, have been used to determine the possibility of reduction of Fe^{3+} to Fe^{2+} by Al-superoxide complex. We have found favorable redox reactions for a variety of aluminum-superoxide species, namely, AlO_2^{2+}, $Al(OH)(O_2^{\bullet})^+$ and $Al(OH)_2(O_2^{\bullet})$. Taking into account previous results supporting the formation of such complexes, our results strongly suggest a Fenton promotion cycle catalyzed by aluminum. In fact, our data can help in the explanation of the experimentally observed pro-oxidant activity of Al, and are coherent with the observed enhanced redox activity of iron in the presence of aluminum.

Acknowledgments

This research was funded by Eusko Jaurlaritza (the Basque Government, GIC 07/85 IT-330-07), the Spanish Ministerio de Ciencia e Innovación (CTQ2011-27374) and the British Engineering and Physical Sciences Research Council (EPSRC EP/J004146/1). The SGI/IZO-SGIker UPV/EHU is acknowledged for computational resources.

References

[1] C. Exley, J. Inorg. Biochem. 97 (2003) 1–7.
[2] C. Exley, Trends Biochem. Sci. 34 (2009) 589–593.
[3] R. Martin, Acc. Chem. Res. 27 (1994) 204–210.
[4] T.L. MacDonald, R.B. Martin, Trends Biochem. Sci. 13 (1988) 15–19.
[5] P. Vasudevaraju Bharathi, M. Govindaraju, A.P. Palanisamy, K. Sambamurti, K.S.J. Rao, Indian J. Med. Res. 128 (2008) 454–556.
[6] L. Tomljenovic, J. Alzheimer's Dis. 23 (2011) 567–598.
[7] S. Murko, R. Milacic, J. Scancar, J. Inorg. Biochem. 101 (2007) 1234–1241.
[8] A.J.A. Aquino, D. Tunega, G. Haberhauer, M.H. Gerzabek, H. Lischka, Phys. Chem. Chem. Phys. 3 (2001) 1979–1985.
[9] A.L. Oliveira de Noronha, L. Guimarães, H.A. Duarte, J. Chem. Theory Comput. 3 (2007) 930–937.
[10] M. Lubin, E. Bylaska, J. Weare, J. Chem. Phys. Lett. 322 (2000) 447–453.
[11] A.J. Sillanpää, J.T. Päivärinta, M.J. Hotokka, J.B. Rosenholm, K.E. Laasonen, J. Phys. Chem. A 105 (2001) 10111–10122.
[12] T. Swaddle, Coord. Chem. Rev. 219 (2001) 665–686.
[13] E. Rezabal, J.M. Mercero, X. Lopez, J.M. Ugalde, J. Inorg. Biochem. 100 (2006) 374–384.
[14] E. Rezabal, J.M. Mercero, X. Lopez, J.M. Ugalde, ChemPhysChem 8 (2007) 2119–2124.
[15] E. Rezabal, J.M. Mercero, X. Lopez, J.M. Ugalde, J. Inorg. Biochem. 101 (2007) 1192–1200.
[16] M.B. Hay, S.C.B. Myneni, J. Phys. Chem. A 112 (2008) 10595–10603.
[17] X. Yang, Q. Zhang, L. Li, R. Shen, J. Inorg. Biochem. 101 (2007) 1242–1250.
[18] J.F. Fan, L.J. He, J. Liu, M. Tang, J. Mol. Model. 16 (2010) 1639–1650.
[19] B.-M. Lu, X.-Y. Jin, J. Tang, S.-P. Bi, J. Mol. Struct. 982 (2010) 9–15.
[20] J. Beardmore, G. Rugg, C. Exley, J. Inorg. Biochem. 101 (2007) 1187–1191.
[21] J. Beardmore, C. Exley, J. Inorg. Biochem. 103 (2009) 205–209.
[22] J.I. Mujika, J.M. Ugalde, X. Lopez, Theor. Chim. Acta 128 (2011) 477–484.
[23] T. Dudev, C. Lim, Annu. Rev. Biophys. 37 (2008) 97–116.
[24] R.B. Martin, Clin. Chem. 32 (1986) 1797–1806.
[25] G.A. Trapp, Kidney Int. 29 (1986) S12.
[26] T.L. Macdonald, W.G. Humphreys, R.B. Martin, Science 236 (1987) 183–186.
[27] J.L. Miller, C.M. Hubbard, B.J. Litman, T.L. Macdonald, J. Biol. Chem. 264 (1989) 243–250.
[28] J.P. Day, J. Barker, L.J.A. Evans, J. Perks, P.J. Seabright, P. Ackrill, J.S. Lilley, P.V. Drumm, G.W.A. Newton, Lancet 337 (1991) 1345.
[29] K. Yamanaka, N. Minato, K. Iwai, FEBS Lett. 462 (1999) 216–220.
[30] W.R. Markesbery, W.D. Ehmann, T.I. Hossain, M. Alauddin, D.T. Goodin, Ann. Neurol. 10 (1981) 511–516.
[31] J.R. McDermott, A.I. Smith, K. Iqbal, H.M. Wisniewski, Neurology 29 (1979) 809–814.
[32] H. Shimizu, T. Mori, M. Koama, M. Sekiya, H. Ooami, Nippon Ronen Igakkai Zasshi 31 (1994) 950–960.
[33] S. Kong, S. Liochev, I. Fridovich, Free Radic. Biol. Med. 13 (1992) 79–81.
[34] A. Khan, J.P. Dobson, C. Exley, Free Radic. Biol. Med. 40 (2006) 557–569.
[35] C. Exley, Free Radic. Biol. Med. 36 (2004) 380–387.
[36] S. Fukuzumi, K. Ohkubo, Chem. Eur. J. 6 (2000) 4532–4535.
[37] S. Fukuzumi, J. Phys. Org. Chem. 15 (2002) 448–460.
[38] S. Fukuzumi, H. Ohtsu, K. Ohkubo, S. Itoh, H. Imahori, Coord. Chem. Rev. 226 (2002) 71–80.
[39] J.I. Mujika, F. Ruipérez, I. Infante, J.M. Ugalde, C. Exley, X. Lopez, J. Phys. Chem. A 115 (2011) 6717–6723.
[40] M.J. Frisch, G.W. Trucks, H.B. Schlegel, G.E. Scuseria, M.A. Robb, J.R. Cheeseman, G. Scalmani, V. Barone, B. Mennucci, G.A. Petersson, H. Nakatsuji, M. Caricato, X. Li, H.P. Hratchian, A.F. Izmaylov, J. Bloino, G. Zheng, J.L. Sonnenberg, M. Hada, M. Ehara, K. Toyota, R. Fukuda, J. Hasegawa, M. Ishida, T. Nakajima, Y. Honda, O. Kitao, H. Nakai, T. Vreven, J.A. Montgomery, J.E. Peralta Jr., F. Ogliaro, M. Bearpark, J.J. Heyd, E. Brothers, K.N. Kudin, V.N. Staroverov, R. Kobayashi, J. Normand, K. Raghavachari, A. Rendell, J.C. Burant, S.S. Iyengar, J. Tomasi, M. Cossi, N. Rega, J.M. Millam, M. Klene, J.E. Knox, J.B. Cross, V. Bakken, C. Adamo, J. Jaramillo, R. Gomperts, R.E. Stratmann, O. Yazyev, A.J. Austin, R. Cammi, C. Pomelli, J.W. Ochterski, R.L. Martin, K. Morokuma, V.G. Zakrzewski, G.A. Voth, P. Salvador, J.J. Dannenberg, S. Dapprich, A.D. Daniels, O. Farkas, J.B. Foresman, J.V. Ortiz, J. Cioslowski, D.J. Fox, Gaussian 09 Revision A.1. Gaussian Inc., Wallingford CT, 2009.
[41] A.D. Becke, J. Chem. Phys. 98 (1993) 5648–5652.
[42] A.D. Becke, Phys. Rev. A 38 (1988) 3098–3100.
[43] C. Lee, W. Yang, R.G. Parr, Phys. Rev. B 37 (1988) 785–789.
[44] S.H. Vosko, L. Wilk, M. Nusair, Can. J. Phys. 58 (1980) 1200–1211.
[45] C. Adamo, V. Varone, J. Chem. Phys. 110 (1999) 6158–6170.
[46] Y. Zhao, D.G. Truhlar, Theor. Chim. Acta 120 (2008) 215–241.
[47] M. Douglas, N.M. Kroll, Ann. Phys. (N.Y.) 82 (1974) 89–155.
[48] B.A. Hess, Phys. Rev. A 33 (1986) 3742–3748.
[49] B.O. Roos, P.R. Taylor, P.E.M. Siegbahn, Chem. Phys. 48 (1980) 157–173.
[50] P.E.M. Siegbahn, A. Heiberg, B.O. Roos, B. Levy, Phys. Scr. 21 (1980) 323–327.
[51] P.E.M. Siegbahn, A. Heiberg, J. Almlöf, B.O. Roos, J. Chem. Phys. 74 (1981) 2384–2397.
[52] K. Andersson, P.-Å. Malmqvist, B.O. Roos, A.J. Sadlej, K. Wolinski, J. Phys. Chem. 94 (1990) 5483–5488.
[53] K. Andersson, P.-Å. Malmqvist, B.O. Roos, J. Chem. Phys. 96 (1992) 1218–1227.
[54] K. Andersson, B.O. Roos, Chem. Phys. Lett. 191 (1992) 507–514.
[55] N. Forsberg, P.-Å. Malmqvist, Chem. Phys. Lett. 274 (1997) 196–204.
[56] F. Aquilante, L. De Vico, N. Ferré, G. Ghigo, P.-Å. Malmqvist, P. Neogrády, T.B. Pedersen, M. Pitoňák, M. Reiher, B.O. Roos, L. Serrano-Andrés, M. Urban, V. Veryazov, R. Lindh, J. Comput. Chem. 31 (2010) 224–247.
[57] B.O. Roos, R. Lindh, P.-Å. Malmqvist, V. Veryazov, P.-O. Widmark, J. Phys. Chem. A 109 (2005) 6575–6579.
[58] B.O. Roos, R. Lindh, P.-Å. Malmqvist, V. Veryazov, J. Phys, J. Phys. Chem. A 108 (2005) 2851–2858.
[59] P.-O. Widmark, P.-Å. Malmqvist, B.O. Roos, Theor. Chim. Acta 77 (1990) 291–306.
[60] V. Barone, M. Cossi, J. Tomasi, J. Comput. Chem. 19 (1998) 404–417.
[61] V. Barone, M. Cossi, J. Tomasi, J. Chem. Phys. 107 (1997) 3210–3221.
[62] M. Cossi, V. Barone, R. Cammi, J. Tomasi, J. Chem. Phys. Lett. 255 (1996) 327–335.
[63] E. Cances, B. Mennucci, J. Tomasi, J. Chem. Phys. 107 (1997) 3032–3041.
[64] A.V. Marenich, C.J. Cramer, D.G. Truhlar 113 (2009) 6378–6396.
[65] C.J. Cramer, Essentials of Computational Chemistry. Theories and Models, Wiley, 2004.
[66] J. Li, C.L. Fischer, J.L. Chen, D. Bashford, L. Noodleman, Inorg. Chem. 35 (1996) 4694–4702.

[67] C. Exley, Coord. Chem. Rev. 256 (2012) 2142–2146.
[68] M. Lavados, M. Guillón, M.C. Mujica, L.E. Rojo, P. Fuentes, R.B. Maccioni, J. Alzheimer's Dis. 13 (2008) 225–232.
[69] M.A. Smith, X. Zhu, M. Tabaton, G. Liu, D.W. McKeel, M.L. Cohen, X. Wang, S.L. Siedlak, T. Hayashi, M. Nakamura, A. Nunomura, G. Perry, J. Alzheimer's Dis. 19 (2010) 363–372.
[70] E.Y. Yang, S.X. Guo-Ross, S.C. Bondy, Brain Res. 839 (1999) 221–226.
[71] J.M.C. Gutteridge, G.J. Quinlan, I. Clark, B. Halliwell, Biochem. Biophys. Acta 835 (1985) 441–447.
[72] P.I. Oteiza, Arch. Biochem. Biophys. 308 (1994) 374–379.
[73] E. Fach, W.J. Waldman, M. Williams, J. Long, R.K. Meister, P.K. Dutta, Environ. Health Perspect. 110 (2002) 1087–1096.
[74] J.F. Colingwood, A. Mikhaylova, M. Davidson, C. Batich, W.J. Streit, J. Terry, J. Dobson, J. Alzheimer's Dis. 7 (2005) 267–272.
[75] Q. Pankhurst, D. Hautot, N. Khan, J. Dobson, J. Alzheimer's Dis. 13 (2008) 49–52.
[76] J.J. Gallagher, M.E. Finnegan, B. Grehan, J. Dobson, J.F. Collingwood, M.A. Lynch, J. Alzheimer's Dis. 28 (2012) 147–161.